Moscow, 30 May to 9 June 1966

morning review lectures of the second international oceanographic congress

(including three in the original French text)

unesco

Published in 1969 by the United Nations
Educational, Scientific and Cultural Organization
Place de Fontenoy, 75 Paris-7e
Printed by Imprimerie Berger-Levrault

Printed in France
SC/NS.67/D.59/AF

K. Hasselmann

The sea surface

Introduction

The frequency spectrum of a typical sea surface record displays two prominent energy bands (Fig. 1): the tides, concentrated in discrete lines around the harmonics of 1 cycle per day, and wind waves, in the continuous band from about 0.05 to 1 cycle per second. The root mean square displacement for each band is of the order of a few metres, but the energies can vary considerably with location and wind conditions. Separating these bands is a broad region of very low energy representing a total root mean square displacement of a few centimetres, which is probably produced by non-linear 'surf beat' interactions between wind waves. The tidal lines are superimposed on a continuum of meteorological origin which continues down to still lower frequencies. The over-all distributions are similar for both deep and shallow water. The stronger non-linearities in shallow water tend to enhance the higher tidal harmonies and the surf beat continuum, and the low-frequency side of the wind wave band is reduced by bottom friction.

We shall be able to consider here only the wind wave continuum. Most investigations of wind waves have centred around two interrelated problems: the prediction of the wave spectrum at any time and position in the ocean, and the analysis of the physical processes which determine the local energy balance of the waves.

Wave prediction

The prediction of the wave spectrum generated at a given time and position in the ocean by a given wind field is a problem of radiative transfer. As input to the problem we need to know the local energy transfer rates, so that the analysis

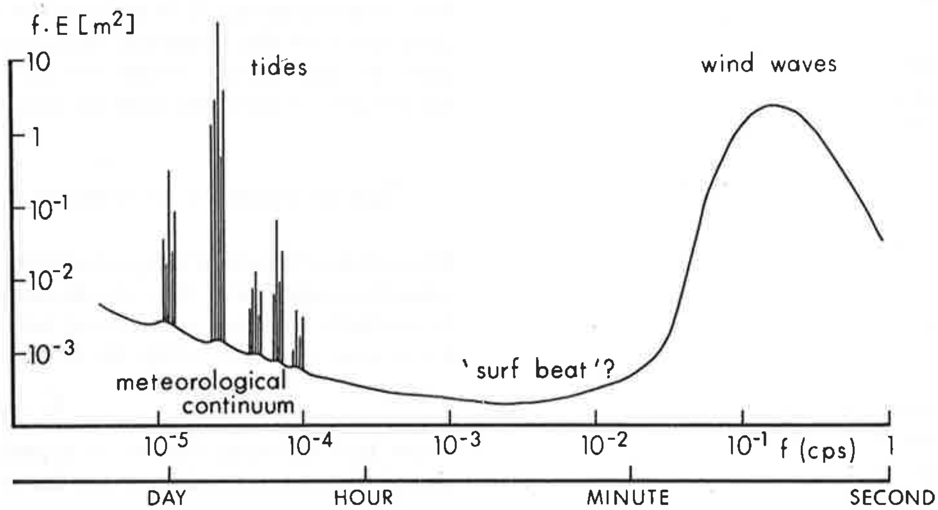

FIG. 1. Spectrum of the sea surface. The spectrum $E(f)$ is multiplied by the frequency f to obtain the spectral density E (log f), in accordance with the logarithmic frequency plot.

of the physical processes which determine these is clearly an essential part of the complete prediction problem. We shall assume here, however, that the transfer expressions are given. In practice, the problem may be approached in a semi-empirical manner by introducing first an empirical expression for the net local transfer and successively amending the expression as improved observations or theoretical relations become available.

For a complete description of the sea surface we need a two-dimensional spectrum describing the distribution of wave energy with respect to both frequency and propagation direction. It is convenient to use the spectral distribution $F(\mathbf{k})$ in the wave number plane. The local rate of change of the spectrum is then given by the radiative transfer, or energy balance equation (Dorrestein, 1960; Hasselmann, 1960).

$$\frac{DF}{Dt}(\mathbf{k};\mathbf{x},t) = \frac{\partial F}{\partial t} + x_1\frac{\partial F}{\partial x_1} + k_1\frac{\partial F}{\partial k_1} = G. \tag{1}$$

Here DF/Dt is the rate of change of the spectrum along the path of a wave group in **x**-**k** phase space, as determined by the Hamiltonian equations $x_i = \partial\omega/\partial k_i$, $k_i = (\partial\omega/\partial x_i)$ where $\omega = \omega\,(\mathbf{k},\mathbf{x})$ is the frequency. G is the net local energy transfer to the spectrum at **k**, which we shall see is a functional of the entire spectrum and the atmospheric boundary layer.

The implicit solution of equation (1) for a given wave group is obtained by integrating along the path of the group in phase space,

$$F(\mathbf{k},\mathbf{x},t) = F(k_0,x_0,t_0) + \int_{t_0}^{t} G(\mathbf{k}(t'),\mathbf{x}(t'),t')dt'.$$

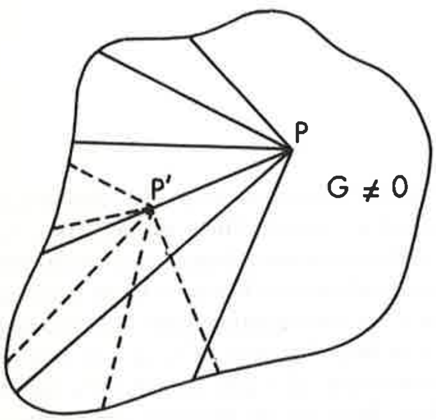

Fig. 2. Ray paths involved in the integration of the radiative transfer equation (1).

The complete spectrum at $(\mathbf{x}, t)$ is then obtained by integrating along all rays that terminate in **x** at time t (Fig. 2). Since G is a functional of the entire spectrum, the integral can be evaluated only if we know the entire spectrum at each point P' on each ray. This, again, involves integration along all rays that terminate in P-, and so on. It follows that all rays of the field are coupled, and it is impossible to determine the spectrum at any one point in the ocean without simultaneously determining the entire spectral field in the region in which G is non-zero. This is a common feature of most transfer problems. Similar problems have been treated successfully in reactor theory and astrophysics by numerical techniques. In our case the transfer equations are generally more complicated (the fields exhibit less symmetry and the functional G is non-linear), but with present-day computers numerical procedures appear feasible. Recent advances in this direction by Gelci and Cazale (1962), Baer (1962), Pierson and Tick (1965) and others look very promising. It is perhaps not too optimistic to predict that wave forecasts based on the numerical integration of the transfer equation will in a few years become routine. Much will depend, however, on our success in clarifying the processes which determine the local transfer rates.

Local transfer processes

The common feature of many wind wave interactions can be explained by V. Laue's refraction experiment (Fig. 3). An incident plane wave of wave number $\mathbf{k}_1$ can be partially refracted by a crystal lattice into a plane wave of wave number $\mathbf{k}_3$ if the wave numbers satisfy the Bragg condition

$$\mathbf{k}_3 = \mathbf{k}_1 + \mathbf{k}_2 \tag{2}$$

where $\mathbf{k}_2$ is the wave number of a periodic set of lattice planes. If the lattice is moved with constant velocity c_2 in the direction of $\mathbf{k}_2$, the incident radiation suffers

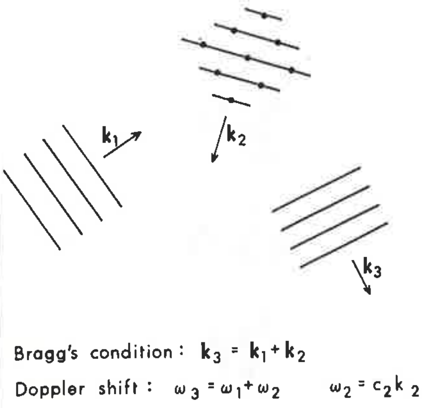

FIG. 3. Scattering of a plan wave of wave number k_1 and frequency ω_1 into another wave of wave number k_3 and frequency ω_3 by a periodic disturbance (for example, crystal lattice) of wave number k_2 moving with velocity c_2.

a Doppler shift $\omega_2 = c_2k_2$ on reflection at the lattice planes, so that the frequency of the refracted wave is

$$\omega_3 = \omega_1 + \omega_2 \tag{2}$$

The conditions (2) and (3) follow from interference considerations and are independent of the form of interaction between the incident radiation and the periodic disturbance which gives rise to the refracted wave. They apply equally to the case in which the disturbance is due to another plane wave rather than a moving lattice. The equations then represent the interaction conditions for the scattering of two waves (1) and (2) into a third wave (3).

Since the same plane wave can also be represented by negative values of the frequency and wave number, the interaction conditions may be written with arbitrary sign combinations of frequencies and wave numbers. It follows then that if waves (1) and (2) can scatter into (3), (3) and (2) can scatter into (1), and (3) and (1) into (2).

Similarly, n waves can interact if

$$\mathbf{k}_n = \sum_{j=1}^{n-1} s_j k_j$$

$$\omega_n = \sum_{j=1}^{n-1} s_j \omega_j, \text{ where } s_j = \pm 1.$$

It is convenient to represent the scattering of energy from $n - 1$ waves into a wave n by a 'Feynman' diagram, in which the interacting wave components are represented by their wave number vectors (Hasselmann, 1966). Negative signs in the interaction conditions are associated with 'anti-wave' components, which are denoted by cross-stroked arrows. Each diagram can be associated with a particular term in the perturbation analysis of the interacting fields. If the wave fields are random, the Feynman diagrams may be interpreted as collision diagrams in a particle picture and thereby indicate the rate and direction in which energy (ω) and momentum (**k**) is transferred between the interacting components.

The diagrams can also be used to describe interactions between wave fields and periodic disturbances associated with non-wave fields, such as the Fourier components of a turbulence field. In this case the particle picture is not valid, but an essential feature of the diagrams is retained: the rate of change of energy of any wave component in a diagram is proportional to the product of the spectral densities of the incoming components.

Let us consider, for example, the interactions between gravity waves (g) and the atmosphere. The atmospheric boundary layer consists of a mean flow and fluctuating turbulent field (t).

Since the mean flow is independent of the horizontal co-ordinates and time it has zero wave-number and frequency. It does not appear in the Feynman diagrams, but it affects the interaction coefficients in the diagram vertices. The complete set of lowest order interactions involving a total of not more than three components are then characterized by the diagrams in Figure 4.

The first interaction $g \rightarrow g$ (Fig. 4(a)) represents Miles' (1957) mechanism of an unstable coupling between the waves and the mean boundary layer flow. This yields an energy transfer of the form

$$DF/Dt = \beta F \tag{4}$$

where β is a function of the mean profile. The wave growth is exponential.

The three interactions $t \rightarrow g$, $tt \rightarrow g$ and $t\bar{t} \rightarrow g$ in Figure 4(b) correspond to Phillips' (1957) mechanism of wave generation through random turbulent pressure fluctuations p. The interactions can be represented more simply by the

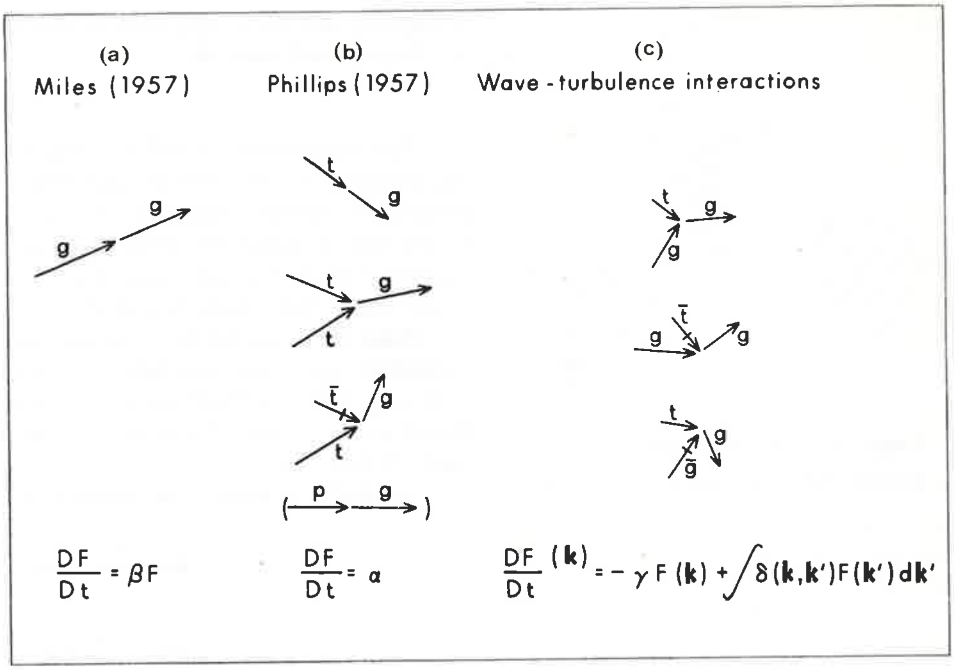

FIG. 4. Interactions between gravity waves (g) and turbulence (t) in the atmospheric boundary layer.

linear interaction diagram $p \rightarrow g$, but the pressure field is itself a derived field which is generated by the turbulent velocity interactions shown in the figure. The energy transfer is given by

$$DF/Dt = \alpha \tag{5}$$

where α is proportional to the spectrum of the turbulent pressure fluctuations at the wave number and frequency of the waves. The wave growth is linear.

The remaining interactions $gt \rightarrow g$, $g\bar{t} \rightarrow g$ and $\bar{g}\bar{t} \rightarrow g$ (Fig. 4(c)) have not been considered previously. They lead to an energy transfer of the form

$$\frac{DF(\mathbf{k})}{Dt} = -\gamma F(\mathbf{k}) + \int \delta(\mathbf{k},\mathbf{k}')F(\mathbf{k}')d\mathbf{k}' \tag{6}$$

where γ and δ are linear functionals of the turbulent velocity spectrum. The wave growth depends on γ and δ, which are difficult to predict on the basis of existing turbulence measurements. It appears probable that the waves grow quasi-exponentially at first and then approach an asymptotic equilibrium value in which the terms on the right hand side of equation (6) balance each other.

Interactions between the waves themselves also produce an appreciable energy transfer (Fig. 5). At least four components are necessary to conserve both energy and momentum (Phillips, 1960). The energy transfer is given by

$$\frac{DF(\mathbf{k})}{Dt} = \int K_1 F(\mathbf{k}')F(\mathbf{k}'')F(\mathbf{k}\text{-}\mathbf{k}'\text{-}\mathbf{k}'')d\mathbf{k}'d\mathbf{k}'' - F(\mathbf{k})\int K_2 F(\mathbf{k}')F(\mathbf{k}'')d\mathbf{k}'d\mathbf{k}'' \tag{7}$$

where K_1 and K_2 are known kernels (Hasselmann, 1960, 1962). The energy transfer is mainly from medium frequencies to higher frequencies, with a weak flux also to low frequencies.

Further interactions produce scattering into internal gravity waves, seismic waves, and the low frequency surf beat continuum. Although important for the coupled fields, their effect on the energy balance of the wind wave spectrum is probably negligible.

The total energy balance is obtained by summing over the transfer rates of all processes. Apart from the processes considered above, this includes the energy

FIG. 5. Fourth order interactions between gravity wave components g.

wave - wave interactions

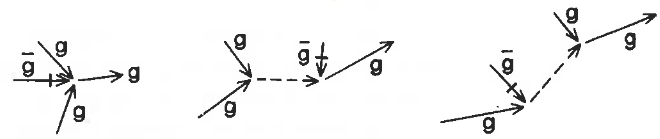

$$\frac{DF(\mathbf{k})}{Dt} = \int K_1 F(\mathbf{k}')F(\mathbf{k}'')F(\mathbf{k}'-\mathbf{k}''-\mathbf{k})\, d\mathbf{k}'d\mathbf{k}'' - F(\mathbf{k})\int K_2 F(\mathbf{k}')F(\mathbf{k}'')\, d\mathbf{k}'d\mathbf{k}''$$

losses due to wave breaking, small scale turbulence and, in shallow water, bottom friction.

Virtually nothing is known of the losses due to wave breaking and turbulence. The dissipation due to bottom friction is normally estimated by evaluating the mean work $<\mathbf{T}\,.\,\mathbf{u}>$ done by an approximate bottom stress $\mathbf{T} = -\, c_f\, \rho\, \mathbf{u}|\mathbf{u}|$ (with constant c_f) against a bottom velocity $\mathbf{u}$. This yields a quasi-linear spectral dissipation of the form

$$DF/Dt = -\, c_f K_{ij} k_i k_j F \qquad (8)$$

where the anisotropic tensor coefficient K_{ij} is a functional of the entire spectrum. The decay rate is slightly slower than exponential.

Comparison with observations

Most wave observations have been made at single stations and unfortunately give little insight into the energy balance of the spectra. Only a few measurements of the rate of growth or decay of waves have been attempted.

Observations of the growth of waves of 3.3 second period by Snyder and Cox (1966) indicate that the initial growth stage is linear. The growth rate is consistent with Phillips' theory, if pressure measurements made on land by Priestley (1965) are assumed to apply also to the ocean. The linear phase is followed by a more rapid exponential growth, which accounts for most of the wave energy. The exponential growth is almost an order magnitude larger than that predicted by Miles, or by the earlier theory of Jeffreys (1925). This naturally suggests the remaining wave-turbulence interactions, Figure 4(c), as the main source of wind waves. The qualitative features of the wave-turbulence appear to be in general agreement with the observations, but a quantitative test must await more detailed measurements of the turbulent structure in the boundary layer, including, in particular, the spectra of vertical correlations of the velocity components.

An interesting feature of the wave-turbulence interactions is that they include a term representing a possible transfer of energy from the waves back to the boundary layer. Hence an equilibrium of the high-frequency part of the spectrum is conceivable without having to invoke a strong dissipative mechanism to balance the energy transfer from the atmosphere to waves. This may have bearing on estimates of the net transfer of momentum from the atmosphere to ocean currents via waves (cf. Snyder and Cox, 1966).

The decay of ocean swell over large distances in the Pacific ocean has been measured by Snodgrass *et al.* (1966). An appreciable decay was observed only in the first 1,000 km to the lee of the generating area. The main features of the decay could be explained by the energy transfer due to non-linear wave interactions.

The attenuation due to bottom friction has been determined by Collins and Bretschneider from measurements made in the Gulf of Mexico (Hasselmann, Collins and Bretschneider, in preparation). Walden *et al.* (1965) have made similar measurements in the German Bight. Collins and Bretschneider's measurements are in agreement with the attenuation computed according to equation (8).

Conclusion

The recent years have seen considerable progress in our understanding of the basic physical processes which determine the energy distribution in the wind-wave continuum. Most of the processes involving linear or weakly non-linear interactions, both between waves and the atmosphere and between the waves themselves, have been clarified. More detailed observations are now needed to fill the gap created by the strong interactions, where rapid theoretical progress is not to be expected. This concerns primarily the turbulent velocity field of the boundary layer and the effects of waves breaking. To test existing theories we also need further wave observations designed specifically to determine not only the wave spectra, but also the rates of change of the spectra in both space and time.

References

Baer, L. 1962. *An experiment in numerical forecasting of deep water ocean waves.* Lockhead Missiles and Space Division. (LMSC 801296.)

Dorrestein, R. 1960. Simplified method of determining refraction coefficient for sea waves. *J. geophys. Res.*, **65**, p. 637-42.

Gelci, R.; Cazale H. 1962. Une équation synthétique de l'évolution de l'état de la mer. *J. Méch. Phys. Atmosph.*, **16**, p. 15-41.

Hasselmann, K. 1960. Grundgleichungen der Seegangsvoraussage. *Schiffstechnik*, **7**, p. 191-5.

——. 1962. On the non-linear energy transfer in a gravity wave spectrum. 1, General theory. *J. Fluid Mech.*, **12**, p. 481-500.

——. 1966. Feynman diagrams and interactions rules of wave-wave scattering processes. *Rev. Geophys.*, **4**, p. 1-32.

Jeffreys, H. 1925. On the formation of water waves by wind. *Proc. Roy. Soc.*, series A, vol. 107, p. 189-206.

Miles J. W. 1957. On the generation of surface waves by shear flows. *J. Fluid Mech.* **3**, p. 185-204.

Phillips, O. M. 1957. On the generation of waves by turbulent wind. *J. Fluid Mech.*, **2**, p. 417-45.

——. 1960. On the dynamics of unsteady gravity waves of finite amplitude. 1, The elementary interactions. *J. Fluid Mech.*, **9**, p. 193-217.

Pierson, W. J., Jr.; Tick, L. J. 1965. The accuracy and potential uses of computer based wave forecasts and hindcasts for the North Atlantic. *Proc. second U.S. Navy Symp. Milit. Ocean*, vol. 1, p. 69-82.

Priestley, J. T. 1965. Correlation studies of pressure fluctuations on the ground beneath a turbulent boundary layer. *Nat. Bur. Stand. Rep. 8942*, 92 p.

Snodgrass, F. E.; Groves, G. W.; Hasselmann, K. F.; Miller, G. R.; Munk, W. H.; Powers, W. H. 1966. Propagation of ocean swell across the Pacific. *Phil. Trans. Roy. Soc.*, series A, vol. 259, p. 431-97.

Snyder, R. L.; Cox, C. S. 1966. A field study of the wind generation of ocean waves. *J. Mar. Res.* In press.

Walden, W.; Lang, A.; Piest, J. 1965. Gleichzeitige Seegangsmessungen in der deutschen Bucht. *Deutscher Wetterdienst, Seewetteramt, Einzelveröff. Nr. 46.*